

Effect of High Temperature on Steady-State Radiolysis Product Behaviour

N. Yousefi, J.M. Joseph, L.M. Alrehaily, J.C. Wren

Department of Chemistry, Western University, 1151 Richmond Street
London, Ontario, Canada N6A 5B7
(nyousefi@uwo.ca)

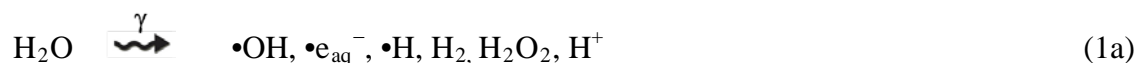
A Master's Level Submission

Summary

Understanding the effect of temperature on the redox environments generated in water by ionizing radiation is important for safety assessments for nuclear reactors. Radiolysis of water creates reactive species that affect the system chemistry and impact the degradation of materials in contact with aqueous phase. Understanding the effect of temperature on the long-term radiolysis helps to determine the steps required to minimize corrosion and enhance reactor lifetime. The radiolytically-produced hydrogen and hydrogen peroxide were measured as a function of irradiation time, pH and dissolved oxygen at room temperature and 150°C. The experimental data were simulated with the steady-state radiolysis kinetic model.

1. Introduction

Some of the operational and safety issues associated with nuclear facilities originate from the impact of water radiolysis on materials performance. The chemically reactive species, shown below, arise as a result of water decomposition when it is exposed to ionizing radiation:[1,2]



Under continuous irradiation, water decomposition products are continuously produced and their concentrations eventually reach steady state. As the radiolysis products are both oxidizing and reducing, having information on steady-state concentrations plays an important role in knowing the redox conditions in the water and consequential corrosion control strategies. Although, continuous water radiolysis is well studied at room temperature [3,4] the effect of temperature on steady-state concentrations is not as well explored. In this paper the results of irradiation of water obtained at 150°C at pHs 6.0 and 10.6 for air-saturated solutions are compared with room temperature results. The experimental results are also compared with computer simulation predictions obtained using a comprehensive water radiolysis kinetic model.

2. Experimental

All the tests used water purified using NANOpure Diamond UV system from Barnstead International. The pHs were adjusted prior to the experiments using sodium hydroxide for room temperature studies and lithium hydroxide for higher temperatures studies. The experiments were performed in sealed quartz vials that were half-filled with water. Prior to a test the water was aerated by purging with high purity air for 1 h. The final step was transfer of a solution into a vial using a syringe and sealing the vial using aluminium crimp caps with PETE silicon septa.

Irradiation was carried out in a ^{60}Co gamma cell (MDS Nordion) which provided the irradiation chamber with a uniform absorption dose rate of $4.5 \text{ kGy}\cdot\text{h}^{-1}$ determined using Fricke dosimetry [1]. Individual vials were taken out of the gamma cell at regular time intervals and the gas and liquid phases were sampled and analyzed for H_2 , using gas chromatography (GC-TCD, 6580, Agilent Technologies), and for H_2O_2 using the UV-VIS spectrophotometric method described in reference [3]. The vials were placed inside an autoclave and heated to the desired temperature prior to irradiation and then the vials and autoclave were irradiated for the desired period of time. The temperature remains constant during the irradiation time. After irradiation the vials were cooled down to room temperature and the analyses of aqueous and gaseous phases were performed.

3. Water Radiolysis Model

The water radiolysis kinetic model consists of a set of elementary chemical reactions that represent production of primary radiolysis species and all of the possible reactions of the radiolysis products with each other, including hydrolysis reactions and acid-base equilibrium. The rate constants of the elementary reactions are well established as a function of temperature [5]. Commercial software FACSIMILIE solves the coupled differential rate equations for the reactions using a numerical integration method. This model has been described in detail in reference [3]. This reaction kinetics model also includes mass transfer of H_2 and O_2 between the gas and aqueous phases as described in reference [6]. This model has been shown to reproduce the steady-state radiolysis of liquid water over a wide range of aqueous conditions at room temperature [3,7,8]. This is the first reported study on the simulation of the steady-state radiolysis experiments as a function of temperature.

4. Results and Discussions

Figure 1 compares the concentrations of $\text{H}_2(\text{g})$ in the headspace observed at 25°C and 150°C . The left hand side of the figure shows the results obtained at pH 6.0 and the right hand side shows the results obtained at pH 10.6. At room temperature $[\text{H}_2(\text{g})]$ increases linearly with time and does not reach a steady state within 5 h, the longest time of irradiation studied. On the other hand, $[\text{H}_2(\text{g})]$ initially increases faster, reaching steady state at 150°C . The results show that the steady-state concentration, $[\text{H}_2(\text{g})]_{\text{SS}}$, is lower at the higher temperature. The $[\text{H}_2(\text{g})]_{\text{SS}}$ at pH 10.6 tends to reach steady state at a longer radiation time compare to pH 6.0. (To date the study at 150°C has been only been performed for tests up to 3 h of irradiation. Work is continuing to include longer-term irradiations).

Also shown in Figure 1 are the calculated $[\text{H}_2(\text{aq})]$ and $[\text{H}_2\text{O}_2(\text{aq})]$. There is very good agreement between the experimental data and the model predictions. The calculated results for $[\text{H}_2(\text{aq})]$ (Figure 1b and 1e) show that the $[\text{H}_2(\text{aq})]$ reaches steady state faster, but the steady-state concentration, $[\text{H}_2(\text{aq})]_{\text{SS}}$, is higher, at 25°C than at 150°C . The different behaviour of the aqueous and gas phase concentrations of H_2 is attributed to the higher equilibrium coefficient ($[\text{H}_2(\text{aq})]_{\text{eq}}/[\text{H}_2(\text{g})]_{\text{eq}}$) for the aqueous-gas phase partitioning of H_2 and the slower mass transfer rate between the two phases at 25°C compared to that at 150°C .

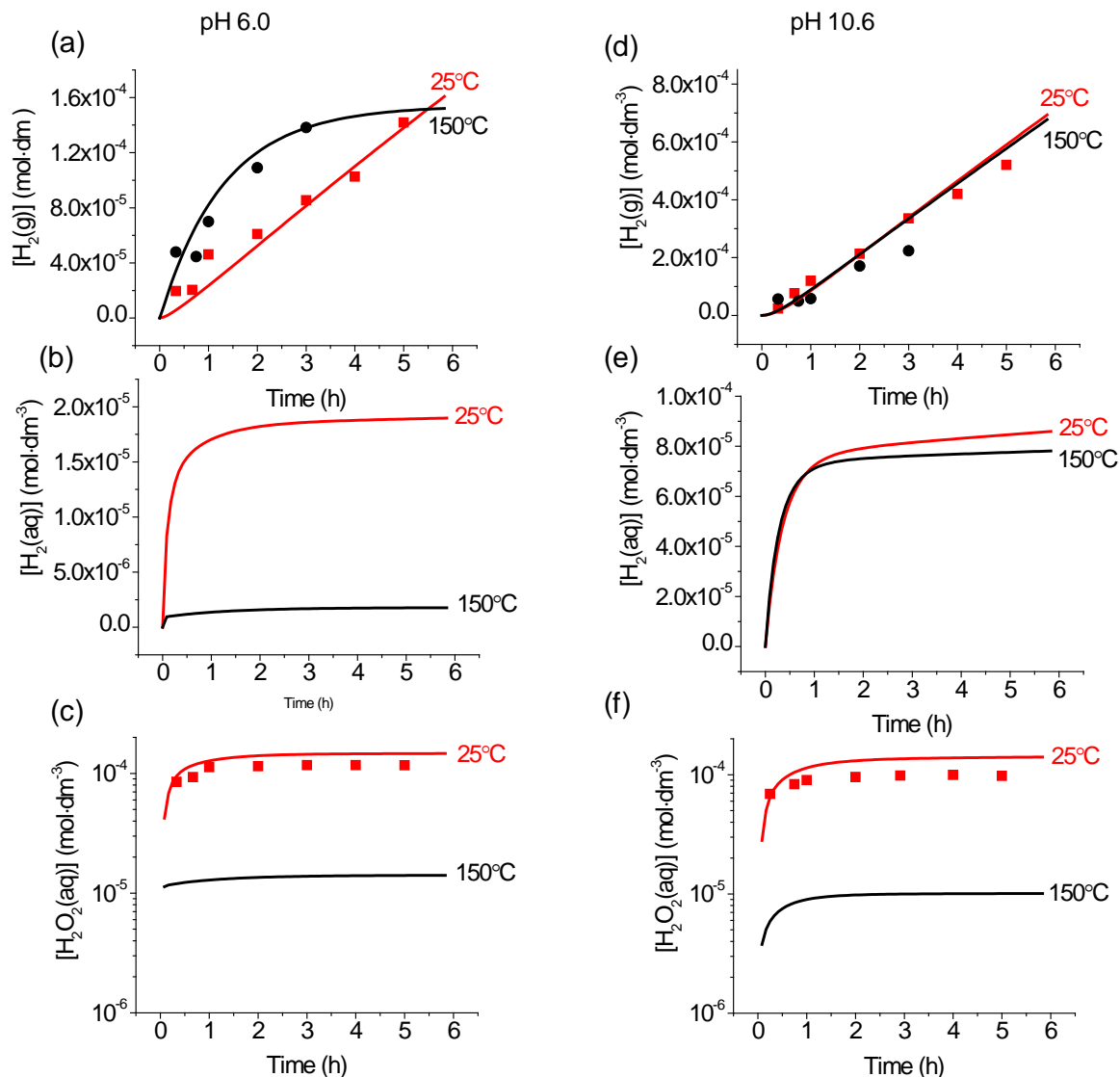


Figure 1: (a) $[H_2(g)]$, (b) $[H_2(aq)]$, (c) $[H_2O_2(aq)]$ for pH 6.0 and (d) $[H_2(g)]$, (e) $[H_2(aq)]$, (f) $[H_2O_2(aq)]$ for pH 10.6 shown as a function of irradiation time for aerated water at 25°C and 150°C. The symbols represent the experimental data and the lines are the computer model simulation results.

The model predicts that the time-dependent behaviours of $[H_2(aq)]$ and $[H_2O_2(aq)]$ are similar, reaching steady state very quickly. This was confirmed experimentally for $H_2O_2(aq)$ at room temperature (Figure 1c and 1f). The model predicts that at 150°C $[H_2O_2(aq)]$ also reaches steady state quickly, but the steady-state concentration, $[H_2O_2(aq)]_{SS}$, is significantly lower (only $\sim 1.2 \times 10^{-5}$ mol·dm⁻³). This is a value that is slightly above our detection limit of 5×10^{-6} mol·dm⁻³. However, we

could not detect any H₂O₂ in water irradiated at 150°C. We attribute this failure to a decrease of the [H₂O₂] caused by thermal decomposition of H₂O₂ that occurred during the cool down period before sampling for H₂O₂ analysis.

The model predicts that the decrease in [H₂O₂(aq)] due to increase in temperature is similar at both pHs. However, the decrease in [H₂(aq)] due to the temperature increase is smaller at pH 10.6 than at pH 6.0. This is attributed to the larger decrease in the concentration of •OH at pH 10.6 – see further discussion below.

We have previously studied the behaviour of water radiolysis products at room temperature under continuous irradiation [3,6,9]. These studies have established that [H₂(aq)] and [H₂O₂(aq)] under continuous irradiation can be approximated by steady-state kinetics. These studies also show that the main production paths for H₂(aq) and H₂O₂(aq) are the primary radiolysis (reactions 1b and 1c). The main path for loss of H₂(aq) is the reaction with •OH (reaction 2) and, in the presence of headspace, partitioning to the gas phase. The main paths for loss of H₂O₂ under aerated conditions are via reaction with •OH (reaction 4) and thermal decomposition (reaction 5). Note that all of the radical species will be in the aqueous phase only and hence, no (g) or (aq) designation is used for them.



The concentrations of [H₂(aq)] and [H₂O₂(aq)] can then be approximated as:

$$[\text{H}_2(\text{aq})] \approx \frac{k_{\text{Rad}}^{\text{H}_2}}{k_2 \cdot [\bullet\text{OH}] + k_3} \quad (6)$$

$$[\text{H}_2\text{O}_2(\text{aq})] \approx \frac{k_{\text{Rad}}^{\text{H}_2\text{O}_2}}{k_4 \cdot [\bullet\text{OH}] + k_5} \quad (7)$$

where $k_{\text{Rad}}^{\text{H}_2} \approx 10^{-6} \cdot G_{\text{H}_2} \cdot D_R \cdot \rho_{\text{H}_2\text{O}}$ and $k_{\text{Rad}}^{\text{H}_2\text{O}_2} \approx 10^{-6} \cdot G_{\text{H}_2\text{O}_2} \cdot D_R \cdot \rho_{\text{H}_2\text{O}}$ represent the zeroth order radiolytic production rates for H₂ and H₂O₂. These rates are determined by the primary radiolysis yields (the G-values in units of μmol·J⁻¹), multiplied by the gamma-radiation dose rate, D_R, in units of Gy·s⁻¹ (or J·kg·s⁻¹) and the density of water (ρ_{H₂O}). The rate constants k₂ and k₄ are the second-order rate constants for reactions (2) and (4), k₃ is the net aqueous-gas mass transfer rate coefficient, and k₅ is the first-order thermal decomposition rate constant for H₂O₂. Note that the net aqueous-gas mass transfer rate coefficient depends on the aqueous-gas partition coefficient and the interfacial mass transfer rate coefficient, both of which are temperature dependent.

To obtain the solutions for $[H_2(aq)]$ and $[H_2O_2(aq)]$ from equations (6) and (7), $[•OH]$ should be known. The radical concentrations are determined by their own set of reactions; production via primary radiolysis and a set of decomposition reaction paths. Due to their high reactivity there are more decomposition reaction paths available for radicals than molecular species [3]. Therefore, simple analytical solutions cannot be obtained and computer model simulations are extensively used to predict the radical and molecular radiolysis products. The computer simulation results show that the analytical expressions (equations 6 and 7), derived based on room temperature studies [3,6,9], still hold at 150°C.

The observed behaviour of $H_2(g)$ as a function of temperature and pH in aerated solutions is consistent with the predictions of the analytical expressions. At higher temperature, $[H_2(aq)]$ and $[H_2O_2(aq)]$ are lower, mainly due to faster interfacial transfer rates (reaction 3) and higher thermal decomposition rates (reaction 5), respectively. The difference in their behaviour as a function of temperature at the two pHs is attributed to their different reactions with $[•OH]$. At pH 10.6, due to the slow reaction of $•e_{aq}^-$ with H^+ , secondary radiolysis products such as $•O_2^-$ can become important in determining the radiolysis behaviour. The increase in $[•O_2^-]$ at the higher pH decreases the $[•OH]$ since $•O_2^-$ reacts catalytically with $•OH$ [3]. The decrease in $[•OH]$, in turn, increases the $[H_2(aq)]$ due to a decrease in the rate of reaction (2). The decrease in $[•OH]$ has a negligible impact on the $[H_2O_2(aq)]$ because thermal decomposition (reaction 5) is the dominant decomposition path at 150°C.

5. Conclusions

Our radiolysis kinetic model reproduces the observed behaviour of $H_2(g)$ production as a function of temperature and this validates the use of model simulations to determine the behaviour of radiolysis products in the aqueous phase. The model analysis shows that $[H_2(aq)]$ and $[H_2O_2(aq)]$ are smaller at 150°C than at room temperature. The smaller concentrations are attributed to the faster aqueous-gas interfacial transfer for $[H_2(aq)]$ and a higher rate for thermal decomposition for $[H_2O_2(aq)]$, respectively. The effect of temperature is less pronounced at pH 10.6 than at pH 6.0. This is attributed to a lower $[•OH]$ at the higher pH.

6. Acknowledgement

The work described herein was funded under the NSERC/AECL Industrial Research Chair in Radiation Induced Processes grant.

7. References

- [1] J.W.T. Spinks, R. J. Woods, *An Introduction to Radiation Chemistry*, Wiley, New York, 1990.
- [2] J.C. Wren, *ACS Symposium Series*, American Chemical Society, Washington, D.C, 2010, 271.
- [3] J.M. Joseph, B.-S. Choi, P.A. Yakabuskie, J.C. Wren, *Radiat. Phys. Chem.*, 77, (2008) 1009.
- [4] A.W. Boyd, M.B. Carver, R.S. Dixon. *Radiat. Phys. Chem.*, 15, (1980) 177.
- [5] A.J. Elliot, D.M. Bartels, AECL 153-127160-450-001, Chalk River, Canada, 2009.
- [6] P.A. Yakabuskie, J.M. Joseph, J.C. Wren, *Radiat. Phys. Chem.*, 79, (2010) 777.
- [7] J.C. Wren, J.M. Ball, *Radiat. Phys. Chem.*, 60, (2001) 577.
- [8] J.C. Wren, G.A. Glowa, *Radiat. Phys. Chem.*, 58, (2000) 341.
- [9] P.A. Yakabuskie, J.M. Joseph, C. Stuart, J.C. Wren, *J. Phys. Chem. A*, 115, (2011) 4270.